

Neutrino Oscillations, SUSY See-Saw Mechanism and Charged Lepton Flavor Violation *

F. Deppisch^a, H. Päs^a, A. Redelbach^a, R. Rückl^a, Y. Shimizu^b

^aInstitut für Theoretische Physik und Astrophysik, Universität Würzburg, D-97074 Würzburg, Germany

^bDepartment of Physics, Nagoya University, Nagoya, 464-8602, Japan

Neutrino oscillations give clear evidence for non-vanishing neutrino masses and lepton-flavor violation (LFV) in the neutrino sector. This provides strong motivation to search for signals of LFV also in the charged lepton sector, and to probe the SUSY see-saw mechanism. We compare the sensitivity of rare radiative decays on the right-handed Majorana mass scale M_R with the reach in slepton-pair production at a future linear collider.

1. Neutrino oscillations

In the recent years a rather unique picture of neutrino mixing has emerged. As can be seen in Fig. 1, large to maximal mixing has been established for solar and atmospheric neutrinos, while the third angle is strongly constrained by reactor measurements. Taking $\theta_{13} = 0^\circ$ and $\theta_{23} = 45^\circ$, the mixing matrix turns out to be of the form

$$V = \begin{pmatrix} \cos \theta_{12} & \sin \theta_{12} & 0 \\ -\frac{\sin \theta_{12}}{\sqrt{2}} & \frac{\cos \theta_{12}}{\sqrt{2}} & \frac{1}{\sqrt{2}} \\ \frac{\sin \theta_{12}}{\sqrt{2}} & -\frac{\cos \theta_{12}}{\sqrt{2}} & \frac{1}{\sqrt{2}} \end{pmatrix}. \quad (1)$$

In the following we focus on the highly favored LMA solution with $\cos \theta_{12} \simeq 0.86$. In addition, the mass squared differences

$$\Delta m_{12}^2 \simeq 6 \times 10^{-5} \text{ eV}^2 \quad (2)$$

$$\Delta m_{23}^2 \simeq 3 \times 10^{-3} \text{ eV}^2 \quad (3)$$

have been deduced from the solar and atmospheric neutrino measurements, respectively. The future long baseline experiments KAMLAND and MINOS, as well as experiments at a neutrino factory and observations of galactic supernovae will significantly improve the knowledge of these parameters.

*Talk presented by R. Rückl at RADCOR 2002, 6th International Symposium on Radiative Corrections, 8-13/09/02, Kloster Banz, Germany

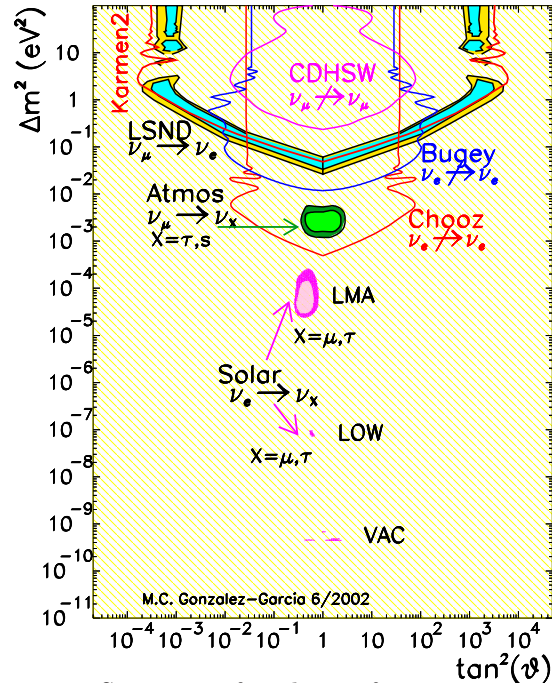


Figure 1. Summary of evidences for neutrino oscillations [1].

2. SUSY see-saw mechanism and slepton mass matrix

If three right-handed neutrino singlet fields ν_R are added to the MSSM particle content, one gets

additional terms in the superpotential [2]:

$$W_\nu = -\frac{1}{2}\nu_R^{cT} M \nu_R^c + \nu_R^{cT} Y_\nu L \cdot H_2. \quad (4)$$

Here, Y_ν is the matrix of neutrino Yukawa couplings, M is the right-handed neutrino Majorana mass matrix, and L and H_2 denote the left-handed lepton and hypercharge +1/2 Higgs doublets, respectively. At energies much below the mass scale of the right-handed neutrinos, W_ν leads to the following mass matrix for the left-handed neutrinos:

$$M_\nu = m_D^T M^{-1} m_D = Y_\nu^T M^{-1} Y_\nu (v \sin \beta)^2. \quad (5)$$

Thus, light neutrino masses are naturally obtained if the mass scale M_R of the matrix M is much larger than the scale of the Dirac mass matrix $m_D = Y_\nu \langle H_2^0 \rangle$ with $\langle H_2^0 \rangle = v \sin \beta$ being the appropriate Higgs v.e.v., $v = 174$ GeV and $\tan \beta = \frac{\langle H_2^0 \rangle}{\langle H_1^0 \rangle}$. The matrix M_ν is diagonalized by the unitary MNS matrix U :

$$U^T M_\nu U = \text{diag}(m_1, m_2, m_3), \quad (6)$$

$$U = \text{diag}(e^{i\phi_1}, e^{i\phi_2}, 1) V(\theta_{12}, \theta_{13}, \theta_{23}, \delta),$$

where ϕ_1 and ϕ_2 are Majorana phases and m_i the light neutrino mass eigenvalues.

The other neutrino mass eigenstates are too heavy to be observed directly. However, they give rise to virtual corrections to the slepton mass matrices that can be responsible for observable lepton-flavor violating effects. In particular, the mass matrix of the charged sleptons is given by

$$m_i^2 = \begin{pmatrix} m_{iL}^2 & (m_{iLR}^2)^\dagger \\ m_{iLR}^2 & m_{iR}^2 \end{pmatrix} \quad (7)$$

with

$$(m_{iL}^2)_{ab} = (m_L^2)_{ab} + \delta_{ab} \left(m_{i_a}^2 + m_Z^2 \cos 2\beta \left(-\frac{1}{2} + \sin^2 \theta_W \right) \right)$$

$$(m_{iR}^2)_{ab} = (m_R^2)_{ab} + \delta_{ab} (m_{i_a}^2 - m_Z^2 \cos 2\beta \sin^2 \theta_W)$$

$$(m_{iLR}^2)_{ab} = A_{ab} v \cos \beta - \delta_{ab} m_{i_a} \mu \tan \beta.$$

When m_i^2 is run from the GUT scale M_X to the electroweak scale one obtains, in mSUGRA,

$$m_L^2 = m_0^2 \mathbf{1} + (\delta m_{L,R}^2)_{\text{MSSM}} + \delta m_L^2 \quad (8)$$

$$m_R^2 = m_0^2 \mathbf{1} + (\delta m_{L,R}^2)_{\text{MSSM}} + \delta m_R^2 \quad (9)$$

$$A = A_0 Y_i + \delta A_{\text{MSSM}} + \delta A, \quad (10)$$

where m_0 is the common soft SUSY-breaking scalar mass and A_0 the common trilinear coupling. The terms $(\delta m_{L,R}^2)_{\text{MSSM}}$ and δA_{MSSM} are well-known flavor-diagonal corrections. In addition, the evolution generates off-diagonal terms which in leading-log approximation are given by [3]

$$\delta m_L^2 = -\frac{1}{8\pi^2} (3m_0^2 + A_0^2) (Y_\nu^\dagger Y_\nu) \ln \left(\frac{M_X}{M_R} \right) \quad (11)$$

$$\delta m_R^2 = 0 \quad (12)$$

$$\delta A = -\frac{3A_0}{16\pi^2} (Y_i Y_\nu^\dagger Y_\nu) \ln \left(\frac{M_X}{M_R} \right). \quad (13)$$

The product of the neutrino Yukawa couplings $Y_\nu^\dagger Y_\nu$ entering these corrections can be determined [2] by inverting (6),

$$Y_\nu = \frac{\sqrt{M_R}}{v \sin \beta} \cdot R \cdot \text{diag}(\sqrt{m_1}, \sqrt{m_2}, \sqrt{m_3}) \cdot U^\dagger, \quad (14)$$

using the neutrino data sketched in section 1 as input, and evolving the result to the unification scale M_X . In the above, we have chosen a basis in which the charged lepton Yukawa couplings are diagonal and have assumed degenerate right-handed Majorana masses. If the unknown complex orthogonal matrix R in (14) is real, it drops out from the product $Y_\nu^\dagger Y_\nu$. Moreover, the latter is also independent of ϕ_1 and ϕ_2 . In what follows we refer to this convenient case which suffices for the present discussion.

For hierarchical (a) and degenerate (b) neutrinos one then obtains

$$(a) (Y_\nu^\dagger Y_\nu)_{ab} \approx \frac{M_R}{v^2 \sin^2 \beta} \times \left(\sqrt{\Delta m_{12}^2} U_{a2} U_{b2}^* + \sqrt{\Delta m_{23}^2} U_{a3} U_{b3}^* \right) \quad (15)$$

$$(b) (Y_\nu^\dagger Y_\nu)_{ab} \approx \frac{M_R}{v^2 \sin^2 \beta} \left(m_1 \delta_{ab} + \frac{\Delta m_{12}^2}{2m_1} U_{a2} U_{b2}^* + \frac{\Delta m_{23}^2}{2m_1} U_{a3} U_{b3}^* \right), \quad (16)$$

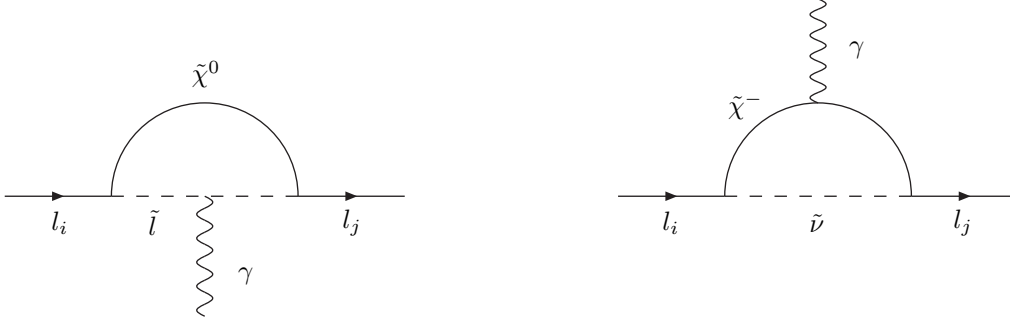


Figure 2. Diagrams for $l_i^- \rightarrow l_j^- \gamma$ in the MSSM

where $\Delta m_{ij}^2 = m_j^2 - m_i^2$ and, in (b), $m_1^2 \gg \Delta m_{23}^2 \gg \Delta m_{12}^2$. Upon diagonalization, the flavor off-diagonal corrections in (8)-(10) generate flavor-violating couplings of the slepton mass eigenstates. It is interesting to note that in the case of degenerate neutrino masses, the lepton-flavor violating effects are suppressed by $\sqrt{\Delta m_{ij}^2}/m_1$ relative to the hierarchical case.

3. Charged lepton flavor violation

If only right-handed neutrinos are added to the standard model, charged lepton-flavor violating processes are suppressed due to the small neutrino masses [4]. However, as outlined above, in supersymmetric models one has new sources of lepton-flavor violation, which may give rise to observable effects (see also [5]).

At low energies, the flavor off-diagonal correction (11) induces the radiative decays $l_i \rightarrow l_j \gamma$. From the photon penguin diagrams shown in Fig. 2 with charginos/sneutrinos or neutralinos/charged sleptons in the loop, one derives decay rates [2, 3]

$$\Gamma(l_i \rightarrow l_j \gamma) \propto \alpha^3 m_i^5 \frac{|(\delta m_L)_{ij}^2|^2}{\tilde{m}^8} \tan^2 \beta, \quad (17)$$

where \tilde{m} characterizes sparticle masses. Because of the dominance of the penguin contributions, the process $\mu \rightarrow 3e$, and also μ - e conversion in nuclei is directly related to $\mu \rightarrow e \gamma$, e.g.,

$$\frac{Br(\mu \rightarrow 3e)}{Br(\mu \rightarrow e \gamma)} \approx \frac{\alpha}{8\pi} \frac{8}{3} \left(\ln \frac{m_\mu^2}{m_e^2} - \frac{11}{4} \right). \quad (18)$$

At high energies, a feasible test of LFV is provided by the process $e^+ e^- \rightarrow \tilde{l}_a^- \tilde{l}_b^+ \rightarrow l_i^- l_j^+ \tilde{\chi}_\alpha^0 \tilde{\chi}_\beta^0$. From the Feynman graphs displayed in Fig. 3, one can see that lepton-flavor violation can occur in production and decay vertices. The helicity amplitudes M_{ab} for the pair production of \tilde{l}_a^- and \tilde{l}_b^+ , and the corresponding decay amplitudes M_a^-, M_b^+ are given explicitly in [6]. The complete amplitude squared is given by

$$\begin{aligned} |M|^2 &= \sum_{abcd} (M_{ab} M_{cd}^*) (M_a^- M_c^{-*}) (M_b^+ M_d^{+*}) \\ &\times \frac{\pi}{2(\tilde{m}_a \Gamma_a + \tilde{m}_c \Gamma_c + i \Delta \tilde{m}_{ac}^2)} \\ &\times \frac{\pi}{2(\tilde{m}_b \Gamma_b + \tilde{m}_d \Gamma_d + i \Delta \tilde{m}_{bd}^2)} \\ &\times (\delta(p_3^2 - \tilde{m}_a^2) + \delta(p_3^2 - \tilde{m}_c^2)) \\ &\times (\delta(p_4^2 - \tilde{m}_b^2) + \delta(p_4^2 - \tilde{m}_d^2)), \quad (19) \end{aligned}$$

where the sum runs over all internal slepton mass eigenstates, $\Delta \tilde{m}_{ac}^2 = \tilde{m}_a^2 - \tilde{m}_c^2$, and the narrow width approximation has been used.

4. Numerical Results

For our numerical investigations we have focussed on the mSUGRA benchmark scenarios proposed in [7] for linear collider studies. These models are consistent with direct SUSY searches, Higgs searches, $b \rightarrow s \gamma$, and astrophysical constraints. Among them, only the benchmark scenarios B, C, G, and I have sleptons which are light enough to be pair-produced at $e^+ e^-$ colliders with c.m. energies $\sqrt{s} = 500 \div 800$ GeV. On the other hand, in the case of the rare lepton de-

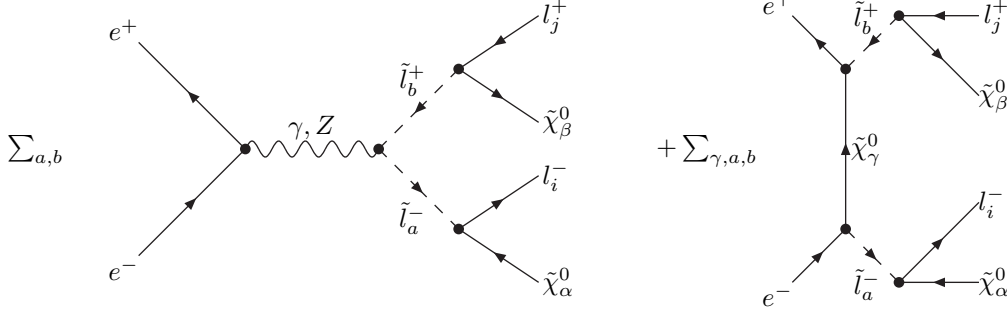


Figure 3. Diagrams for $e^+e^- \rightarrow \tilde{l}_a^- \tilde{l}_b^+ \rightarrow l_i^- l_j^+ \tilde{\chi}_\alpha^0 \tilde{\chi}_\beta^0$

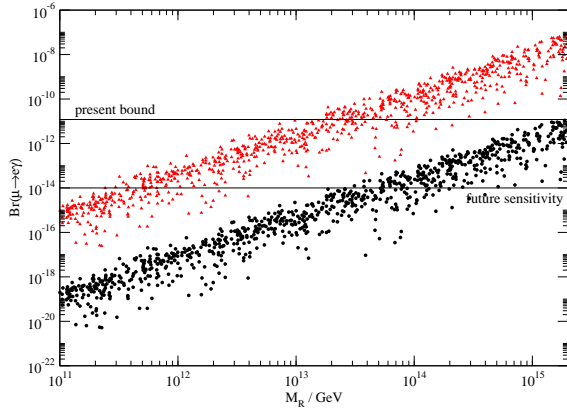


Figure 4. Branching ratio of $\mu \rightarrow e\gamma$ for hierarchical neutrino masses and uncertainties of future neutrino experiments in the mSUGRA scenarios L and H leading to the largest and smallest signals, respectively.

ays, where the SUSY particles only enter virtually, we have investigated all mSUGRA scenarios specified in [7].

For the neutrino input we have taken the global three neutrino LMA fit given in [8] and have varied Δm_{ij}^2 and θ_{ij} within the 90% CL intervals. In order to demonstrate possible future improvements, we have also considered uncertainty intervals as expected from future experiments [9]. For hierarchical neutrinos the lightest neutrino mass is assumed to lie in the interval $m_1 \approx 0 - 0.03$ eV. For degenerate neutrinos we take $m_1 \approx 0.3_{-0.16}^{+0.11}$ eV [9]. The only free parameter is the Majorana mass scale M_R .

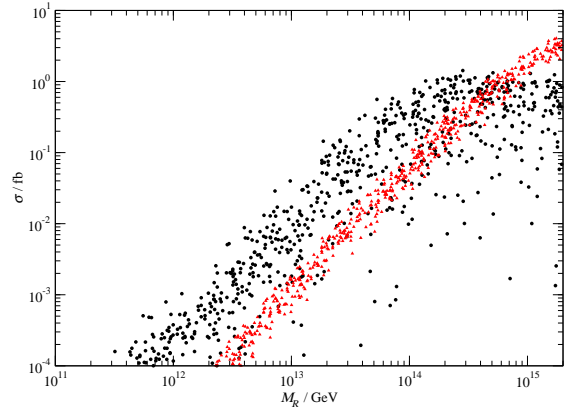


Figure 5. Cross sections for $e^+e^- \rightarrow e^-\mu^+ + 2\tilde{\chi}_1^0$ (circles) and $e^+e^- \rightarrow \mu^-\tau^+ + 2\tilde{\chi}_1^0$ (triangles) at $\sqrt{s} = 500$ GeV for the mSUGRA scenario B and the same neutrino input as in Fig. 4.

Fig. 4 shows the dependence of $Br(\mu \rightarrow e\gamma)$ on M_R for the mSUGRA scenarios L and H, which lead to the largest and smallest branching ratios, respectively, in the set of models considered. One sees that a positive signal between the present bound and the minimum branching ratio observable in the new PSI experiment would imply a value of M_R between $5 \cdot 10^{11}$ GeV and $5 \cdot 10^{15}$ GeV.

In comparison to $\mu \rightarrow e\gamma$ the channel $\tau \rightarrow \mu\gamma$ is less affected by the neutrino uncertainties. On the other hand, with a sensitivity in the range $Br(\tau \rightarrow \mu\gamma) = 10^{-6} \div 10^{-9}$ one can only probe M_R above $2 \cdot 10^{13}$ GeV [9].

In Fig. 5 the cross-sections for $e^+e^- \rightarrow e^-\mu^+ + 2\tilde{\chi}_1^0$ and $e^+e^- \rightarrow \mu^-\tau^+ + 2\tilde{\chi}_1^0$ are plotted versus M_R at $\sqrt{s} = 500$ GeV. The channel $e^-\tau^+ + 2\tilde{\chi}_1^0$

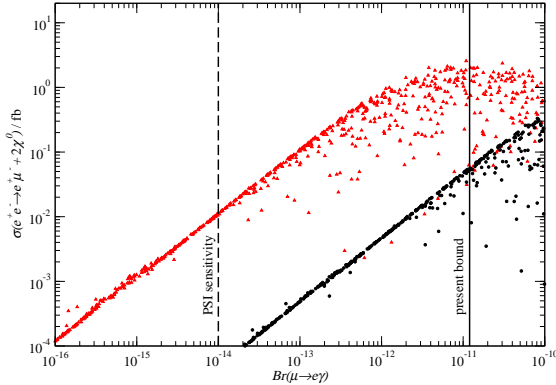


Figure 6. Correlation between $Br(\mu \rightarrow e\gamma)$ and $\sigma(e^+e^- \rightarrow e^-\mu^+ + 2\tilde{\chi}_1^0)$ at $\sqrt{s} = 800$ GeV for the mSUGRA scenarios I (circles) and C (triangles) and the same neutrino input as in Fig. 4.

is strongly suppressed by the small mixing angle θ_{13} , and therefore more difficult to observe.

The standard model background mainly comes from W production in $e^+e^- \rightarrow l_i^- l_j^+ \bar{\nu}_i \nu_j$. With a beam-pipe cut of 10 degrees but no other cuts the cross section for the $e\mu$ final state is roughly 100 fb at $\sqrt{s} = 500$ GeV. The MSSM background is dominated by chargino/slepton production in $e^+e^- \rightarrow l_i^- l_j^+ + 2\tilde{\chi}_1^0 + 2(4)\nu$ with a total cross section of $0.01 \div 0.02$ fb at $\sqrt{s} = 500$ GeV for $l_i^- l_j^+ = e^-\mu^+$. This background should be manageable, as the sparticle properties will be known by the time such an experiment can be performed.

As a final result we point out the very interesting and useful correlation between LFV in the radiative decays and in high-energy slepton-pair production. This is illustrated in Fig. 6 for $Br(\mu \rightarrow e\gamma)$ and $e^+e^- \rightarrow e^-\mu^+ + 2\tilde{\chi}_1^0$. In this comparison the neutrino uncertainties almost drop out, while the sensitivity to the mSUGRA parameters remains.

5. Conclusions

The SUSY see-saw mechanism can be tested by lepton-flavor violating processes involving charged leptons. Here we have concentrated on

the sensitivity of $Br(l_i \rightarrow l_j\gamma)$ and $\sigma(e^+e^- \rightarrow \tilde{l}_a^- \tilde{l}_b^+ \rightarrow l_i^- l_j^+ + \cancel{E})$ on the Majorana mass scale M_R . Assuming the LMA solution for solar neutrino oscillations we have illustrated the impact of the uncertainties in the neutrino parameters. Furthermore, using post-LEP mSUGRA scenarios we have investigated the strong dependence of LFV signals on the mSUGRA parameters. In the case of hierarchical neutrino masses, a measurement of $Br(\mu \rightarrow e\gamma) \approx 10^{-14}$ would probe M_R in the range $3 \cdot 10^{11} \div 4 \cdot 10^{14}$ GeV, depending on the mSUGRA scenario. For degenerate neutrinos a similar signal would require $M_R > 2 \cdot 10^{12}$ GeV. However, if the mSUGRA scenario is known, one may actually be able to determine M_R within a factor of 10. In comparison, a measurement of $Br(\tau \rightarrow \mu\gamma) \approx 10^{-9}$ would imply M_R larger than $2 \cdot 10^{13}$ GeV and, for a given scenario, allow to determine M_R within a factor of 2. Finally, we find that $Br(\mu \rightarrow e\gamma) = 10^{-14} \div 10^{-11}$ implies $\sigma(e^+e^- \rightarrow e^-\mu^+ + 2\tilde{\chi}_1^0) = 10^{-2} \div 1$ fb at $\sqrt{s} = 800$ GeV in the most favorable mSUGRA scenario C.

Acknowledgements

This work was supported by the Bundesministerium für Bildung und Forschung (BMBF, Bonn, Germany) under the contract number 05HT1WWA2.

REFERENCES

1. M. C. Gonzalez-Garcia and Y. Nir, arXiv:hep-ph/0202058.
2. J. A. Casas and A. Ibarra, Nucl. Phys. B **618**, 171 (2001) [arXiv:hep-ph/0103065].
3. J. Hisano and D. Nomura, Phys. Rev. D **59**, 116005 (1999) [arXiv:hep-ph/9810479].
4. S. M. Bilenkii, S. T. Petcov and B. Pontecorvo, Phys. Lett. B **67**, 309 (1977).
5. Talk by J. Illana at this conference.
6. F. Deppisch, H. Päs, A. Redelbach, R. Rückl and Y. Shimizu, in preparation.
7. M. Battaglia *et al.*, Eur. Phys. J. C **22** (2001) 535 [arXiv:hep-ph/0106204].
8. M. C. Gonzalez-Garcia, M. Maltoni, C. Pena-

- Garay and J. W. F. Valle, Phys. Rev. D **63**, 033005 (2001) [arXiv:hep-ph/0009350].
9. F. Deppisch, H. Päs, A. Redelbach, R. Rückl and Y. Shimizu, arXiv:hep-ph/0206122.